Title

Design of a Superconducting 28 GHz Ion Source Magnet for FRIB Using a Shell-Based Support Structure

Journal
IEEE Transactions on Applied Superconductivity, 25(3)

ISSN
1051-8223

Authors
Felice, H
Rochepault, E
Hafalia, R
et al.

Publication Date
2015

DOI
10.1109/tasc.2014.2377730

Peer reviewed

Design of a Superconducting 28 GHz Ion Source Magnet for FRIB Using a Shell-Based Support Structure

H. Felice, E. Rochepault, R. Hafalia, S. Caspi, D. R. Dietderich, S. O. Prestemon,
G. Machicoane, E. Pozdeyev, N. Bultman, and X. Rao

***Abstract*—The Superconducting Magnet Program at the Lawrence Berkeley National Laboratory (LBNL) is completing the design of a 28 GHz NbTi ion source magnet for the Facility for Rare Isotope Beams (FRIB). The design parameters are based on the parameters of the ECR ion source VENUS in operation at LBNL since 2002 featuring a sextupole-in-solenoids configuration. Whereas most of the magnet components (such as conductor, magnetic design, protection scheme) remain very similar to the VENUS magnet components, the support structure of the FRIB ion source uses a different concept. A shell-based support structure using bladders and keys is implemented in the design allowing fine tuning of the sextupole preload and reversibility of the magnet assembly process. As part of the design work, conductor insulation scheme, coil fabrication processes and assembly procedures are also explored to optimize performance. We present the main features of the design emphasizing the integrated design approach used at LBNL to achieve this result.**

***Index Terms*—ECR ion source magnet, NbTi, shell-based support structure.**

I. Introduction

The Superconducting Magnet Program at Lawrence Berkeley National Laboratory is in charge of the design of a 28 GHz NbTi Electron Cyclotron Resonance (ECR) ion source magnet for the Facility for Rare Isotope Beams (FRIB). This high-performance ion source will provide high beam current of heavy ion up to Uranium, making it a key component of the FRIB front-end [1].

Performance of an ECR ion source relies primarily on the plasma density and confinement time. The plasma is produced by ECR heating of the electrons. Higher electronic density is achieved at higher heating frequency. To date, the highest beam currents have been achieved with ECR ion source operating at 24–28 GHz [2]–[4]. To build-up the plasma density, a strong confinement of the plasma is required. It is obtained by means of a magnetic field configuration featuring closed iso-surfaces (iso-B) which have a minimum at the center of the plasma. This configuration is produced by the combination of sextupole and solenoid fields. As the confinement field has to increase with the ECR heating frequency, high intensity sources require high magnetic fields making superconducting magnets a key technology of the high performance source.

In the case of the FRIB ECR source, the expected beam intensities are at the edge of performance being demonstrated by the most advanced ECR sources such as VENUS, in operation at LBNL since 2002 [2]. Given the VENUS reliable performance, the magnetic parameters of the FRIB ECR magnet were maintained as close as possible to the VENUS magnet ones and the "sextupole-in-solenoids" assembly was preserved. However, as part of the design study, the sextupole coil fabrication was re-evaluated to optimize the process. From a magnet assembly standpoint, a shell-based support structure using bladder and keys was implemented [5] allowing for fine tuning of the sextupole preload and for reversibility of the assembly process. Extensively used in the development of the future LHC Interaction Region quadrupoles [6] and [7], bladder and keys technology was also used in the design study of a 56 GHz ECR ion source [8] and [9]. An overview of the design proposed for the FRIB ECR ion source magnet is reported here along with the progress on a sextupole practice coil fabrication.

II. Magnet Parameters

A. Conductor

The FRIB ECR magnet being similar to the VENUS ECR magnet, conductor specifications were defined using experience from the VENUS construction project. The FRIB conductor specifications were based on the conductor performance measured on actual VENUS conductor at the time of the VENUS construction. This set of specification is summarized in Table I. Both the sextupole and the solenoids conductor are rectangular NbTi wires coated with Formvar. The sextupole specifications are particularly stringent as they require high Ic value in spite of the large copper content. In addition, high aspect ratio is preferred for ease of wind-ability. To achieve target dimensions, the wire is rolled to rectangular shape which degrades the RRR.

Manuscript received August 12, 2014; accepted November 19, 2014. Date of publication December 5, 2014; date of current version March 13, 2015. This work was supported by the U.S. Department of Energy, Office of Science under Contract No. DE-AC02-05CH11231 and under Cooperative Agreement DE-SC0000661.

H. Felice, E. Rochepault, R. Hafalia, S. Caspi, D. R. Dietderich, and S. O. Prestemon are with the Lawrence Berkeley National Laboratory, Berkeley, CA 94720 USA (e-mail: hfelice@lbl.gov).

G. Machicoane, E. Pozdeyev, N. Bultman and X. Riao are with the Facility for Rare Isotope Beams, Michigan State University, East Lansing, MI 48824-1321 USA.

Color versions of one or more of the figures in this paper are available online at http://ieeexplore.ieee.org.

Digital Object Identifier 10.1109/TASC.2014.2377730

TABLE I
PROCURED CONDUCTOR PARAMETERS

Parameter	Units	Specifications
SEXTUPOLE NbTi wire		
Bare width / thickness	mm	1.8 / 0.9
Insulation Type		Formvar
Insulation thickness	mm	0.05
Filament diameter	µm	<40
Cu/Sc		3:1 +/-0.3
RRR		>150
Minimum guaranteed Ic at 5T and 4.2 K	A	1080
Minimum guaranteed Ic at 7T and 4.2 K	A	640
SOLENOIDS NbTi wire		
Bare width / thickness	mm	1.57 / 0.88
Insulation Type		Formvar
Insulation thickness	mm	> 0.038
Filament diameter	µm	< 40
Cu/Sc		4:1 +/- 0.5
RRR		>80
Minimum guaranteed Ic at 6T and 4.2 K	A	600

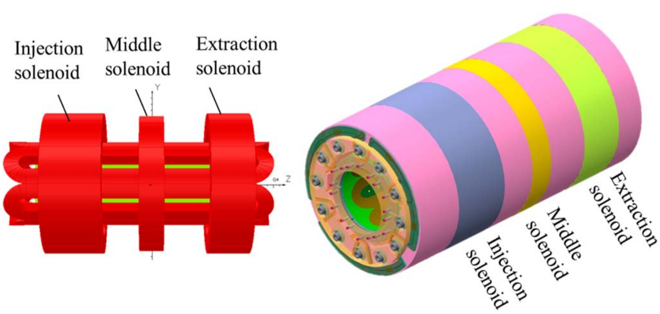

Fig. 1. Left: Sextupole in solenoids configuration—Right: Magnet assembly.

An additional annealing step is required to regain it. Since the Formvar is not compatible with the annealing temperature, the conductor can only be dip-coated at the end of the process. Given the constraints, three vendors were consulted but only one was able to meet all the sextupole conductor specifications.

B. Magnetic Design

The key requirement for the superconducting magnet system of an ECR source is to produce closed iso-B surfaces with a minimum at the center of the plasma made from a combination of multipole field (creating a field gradient radially), typically a sextupole, and solenoid fields. The confinement of the plasma charged particle along the ion source axis is provided by maxima of field produced by an injection and an extraction solenoid (mirror field). A middle solenoid is used with opposite current to provide a mean to adjust the field gradient around the ECR heating surface (Fig. 1). The resonance condition and therefore the heating of the electrons is achieved when the electron cyclotron frequency is equal to the RF frequency. For an RF frequency f in GHz, the required field strength B_{ecr} in Tesla in the ECR source can be determine by:

$$B_{ecr} = \frac{f}{28}. \quad (1)$$

TABLE II
MAGNET PARAMETERS

Parameter	Units	
SEXTUPOLE		
Inner / Outer radius	mm	100 / 136
Endshoe to endshoe length	mm	896
Number of turns		646
Nominal current	A	450
Peak Field at nominal	T	6.6
Temperature margin	K	0.9
Inductance at nominal	H	1.7
Lorentz forces at nominal		
Fx/Fy ss top coil	kN	97 / -294
Fx/Fy ss bottom coil	kN	102 / 312
Fr/Fz injection side end top	kN	-49 / -52
Fr/Fz injection side end bottom	kN	44 / -15
Fr/Fz extraction side end top	kN	37 / 18
Fr/Fz extraction side end bottom	kN	24 / 49
INJECTION SOLENOID		
Inner / Outer radius	mm	170 / 229.46
Length	mm	190.45
Number of turns per layer/layers		112 / 56
Nominal current	A	233
Peak Field at nominal	T	6.15
Inductance	H	13.96
MIDDLE SOLENOID		
Inner / Outer radius	mm	170 / 220.98
Length	mm	78.25
Number of turns per layer/layers		46/48
Nominal current	A	-155
Peak Field at nominal	T	3.4
Inductance	H	2.4
EXTRACTION SOLENOID		
Inner / Outer radius	mm	170 / 229.46
Length	mm	136.05
Number of turns per layer/layers		80/56
Nominal current	A	152
Peak Field at nominal	T	4.1
Inductance	H	8.05

B_{ecr} is equal to 1 T in the case of a 28 GHz ECR source. From there, some empirical scaling laws established by the ECR community [10] allow determining solenoid, sextupole and iso-B field value (all proportional to B_{ecr}) required to achieve 28 GHz operation. In the case of the FRIB ECR source, these requirements at nominal and maximum operation can be summarized as follow:

- Field under the injection solenoid on the axis: 4 T.
- Field under the extraction solenoid on the axis: 2 to 3 T.
- Field in between extraction and injection solenoids: 0.4–0.8 T.
- $B_{sextupole}$ (B_θ at $\theta = 0$, B_r at $\theta = 30$ degree) of the order of 2 T at a radius of 71.85 mm.
- Last closed iso-B greater than 1.75 T.

Due to the asymmetry of the field distribution, the finite element model minimum symmetry is a sextant spanning from -30 to 30 degrees. Solenoids and sextupole geometrical dimensions are summarized in Table II along with the peak field on conductor and other magnetic parameters. With these parameters, nominal and maximum operational field profiles on the axis of the FRIB ECR magnet are consistent with the requirement listed before and can be seen in Fig. 2.

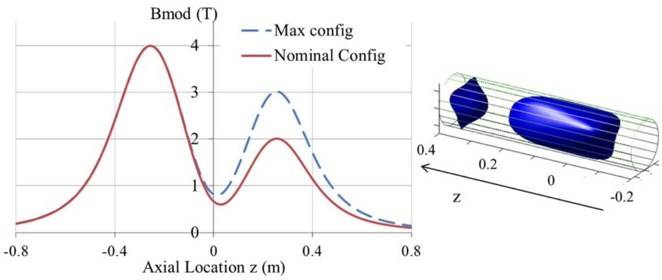

Fig. 2. Left: Field profile on the axis of the ECR—Right: Closed iso-B surface at 1.85 Tin the ECR magnet aperture.

Regarding the radial confinement, to increase the sextupole field in the aperture while limiting the peak field on the conductor, each sextupole coil is wound around a full length iron pole. At a radius of 71.85 mm, a field of 2 T (+/−0.01 T) along a 170 mm long zone is produced. In nominal operation, the highest iso-B surface produced by the combination of the sextupole and solenoid fields within the ion source plasma chamber is 1.85 T and is shown in Fig. 2. In this operating condition, the sextupole temperature margin is 0.9 K and the solenoids temperature margins are 1.5 K, 3 K and 2.7 K for the injection, middle and extraction solenoids. The Lorentz forces produced by such a magnetic configuration on the sextupole are highly asymmetric. In the sextupole, neighboring coil straight sections are subjected to asymmetric forces due to the field produced by the solenoids. In the ends, one coil end out of two is subjected to negative radial forces pushing it radially inward, while the others are subjected to positive radial forces pushing them radially outward. The amplitude of these forces differs between extraction and injection side. A summary of these forces is listed in Table II. The magnet is operating 4.2 K in a LHe bath.

III. Quench Protection

The overall system stored energy is of 625 kJ in nominal operating condition. The sextupole and each of the solenoids are powered independently. Preliminary quench protection study was performed with the program QUENCH [11] was used to compute hot spot temperature and voltage distribution for each component.

Each sextupole coil will be individually protected by a set of back-to-back diodes. In that configuration, the sextupole is self-protected with a peak voltage of 125 V and a hot spot temperature of 150 K. Regarding the solenoids, the injection solenoid seems the most critical with a peak temperature estimated at 260 K and a concerning peak voltage close to 1 kV. Additional analysis is planned for a better assessment of the protection parameters at nominal and maximum operation.

IV. Magnet Assembly and Preload

The magnet assembly process is based on experiences acquired at LBNL on short and long magnet prototypes [6] and [7]. The development of the assembly steps goes hand-in-hand with 2D and 3D FEM mechanical analysis. Assembly, cool-down and excitation are simulated to optimize preload targets and ensure proper pre-stress of the magnet during operation. We present here a summary of the assembly steps and highlights on the mechanical analysis. Deeper analysis and model description can be found in [12].

A. Solenoids Assembly

The three solenoids will be wet-wound using Stycast on a 7075-T6 Aluminum alloy mandrel. The winding will be done under tension (60 MPa) to maintain compression against the mandrel during operation. In addition to the radial forces, the solenoids are subjected to axial Lorentz forces which will tend to separate them. Since axial motion cannot be eliminated, appropriate slip planes are introduced to minimize friction and energy dissipation. A combination of Kapton layers, pre-impregnated E-glass cloth and Teflon or Tedlar layers will provide electrical insulation and minimize friction. Routing of the stabilized solenoids leads will be done tangentially to the winding layers. The solenoids will be reinforced externally by a 10 mm thick banding made of Aluminum wire wound under tension. In the FEM model, the solenoids and reinforcement winding tensions are simulated by imposing displacement between mandrel and solenoids layers and between solenoids outermost layer and banding. The solenoid preload causes the mandrel inner diameter to move inward radially under the solenoids, giving a wavy shape to the mandrel longitudinally, This inward displacement will be quantified during fabrication by performing CMM measurements on the mandrel inner diameter after winding of the solenoids.

B. Sextupole Assembly and Preload

Minimizing conductor motion in superconducting magnets is essential to reduce training and to achieve operational field. In the case of the ECR sextupole, the sextupole pole turns must be in azimuthal compression along the straight section and in axial compression at the ends during excitation. This is achieved by assembling the sextupole coils in six stainless steel pads bolted together. This coil pack sub-assembly is inserted in the mandrel on which the solenoids have been pre-wound. Coil to pad ground plane insulation is ensured by layers of Kapton wrapped around the pads. Additional layers of G10 are glued to the Kapton reinforcing electrical integrity and allowing fine tuning of the coil outer diameter and pad inner diameter matching. Once the coil-pack is inserted in the mandrel, bladders are inserted in between the pads and the mandrel as shown in Fig. 3. The bladders are inflated with pressurized water (∼30 MPa), pre-compressing the coil azimuthally and stretching the mandrel. During that phase, gaps open between the load keys and the mandrel. These gaps are filled with appropriate shimming (∼0.2 mm); the bladders are deflated and removed.

The shimmed load keys maintain the sextupole in azimuthal compression. This step is simulated in the FEM by imposing a displacement of 0.2 mm between load keys and mandrel. Due to the wavy shape of the mandrel, the azimuthal preload on the sextupole is inhomogeneous longitudinally with strong azimuthal compression in the section of the sextupole located under the solenoids and weak azimuthal preload for section which are in between solenoids as seen in Fig. 4.

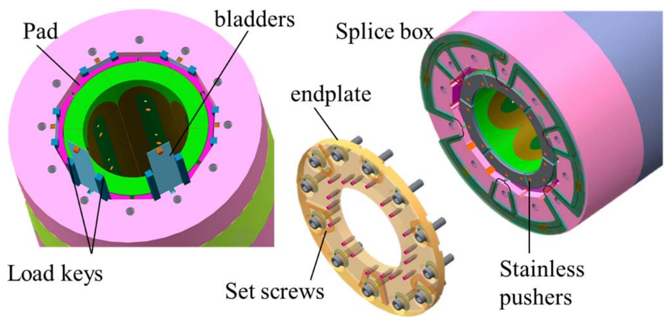

Fig. 3. Views of the magnet assembly.

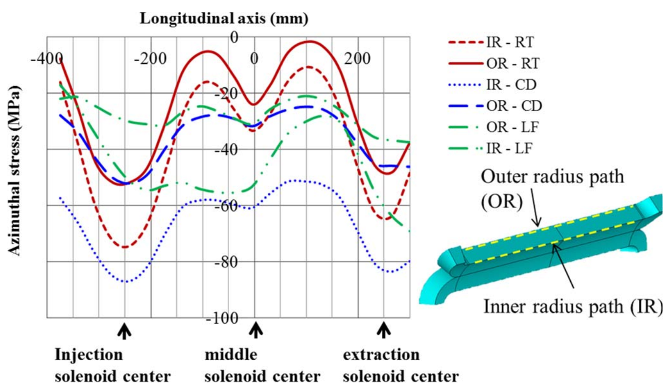

Fig. 4. Azimuthal stress in the sextupole top coil turns in contact with the pole along the straight section on the inner radius (IR) and outer radius (OR) after room temperature preload (RT) and after cool-down (CD) and with Lorentz forces (LF).

During cool-down, the differential thermal contraction between the Aluminum mandrel and the coil pack increases the pre-stress on the sextupole setting its final preload. As shown in Fig. 4, the inhomogeneity is slightly improved and appropriate preload is applied everywhere along the straight section. During excitation, the Lorentz Forces tend to separate the pole turns from the pole piece. This can be seen in Fig. 4, where, while remaining in compression, the pole turns see their azimuthal stress reduced under the effect of the Lorentz forces. Axial support is provided to the sextupole by means of end plates bolted at each end of the mandrel. Contact is made with the end of the sextupole via set screws contacting a 5 mm thick stainless steel pusher plate mounted at the end of the end-shoes. Ground plane insulation is provided by a 2 mm G11 filler sandwiched between the end of the end-shoe and the stainless steel pusher. From cool-down to nominal operation, the coil end remains in compression (10–100 MPa) against the pole piece. The leads of the sextupole will be routed outside of the end-shoes, radially outward and spliced in a G10 splice box (Fig. 3). As pointed out in [2], proper stabilization of the leads is essential to protect them in case of lead quenching. This will be achieved by doubling each of the sextupole leads using identical NbTi conductor.

V. Sextupole Coil Fabrication

As part of the design study, a dry sextupole coil fabrication process is considered to improve the quality of the winding and in particular the coil packing factor. Coils using a small NbTi conductor are usually wet wound making conductor placement inaccurate and, therefore, the total number of turns difficult to control. A dry winding approach can free the winding crew from time constraints due to the stycast working time frame allowing better control of the turn positioning. Moreover, given the concept of the support structure, the matching between the coil outer diameter and the pads inner diameter is essential to ensure proper coil preload. This can be achieved by vacuum-impregnating the coil with Epoxy in a confined cavity. To demonstrate the feasibility of the dry-winding and coil vacuum impregnation concept, a practice sextupole coil is being fabricated at LBNL.

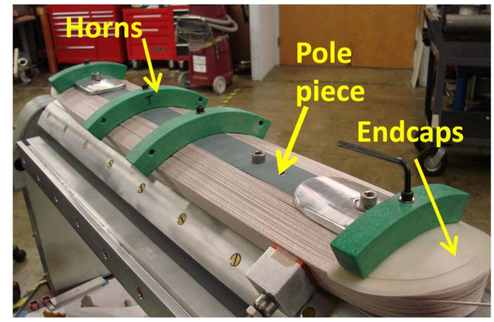

Fig. 5. Practice coil dry wound with green horn and G10 end caps.

Dry winding combined with Epoxy vacuum impregnation requires the presence of glass cloth in the system to provide epoxy wicking, bonding and reinforcement. Given the large amount of turns of this layout, it was found very tedious to insert layer of glass in between layers of conductors. To alleviate this issue, a 50 micron sleeve of E-glass (with starch/oil sizing) was directly braided onto the Formvar insulated conductor eliminating the need for glass cloth during winding. The Formvar insulated practice wire used in the practice coil is 0.96 by 1.96 mm which is slightly different from the nominal wire used in the design (see Table I). Therefore a dedicated layout accounting for the practice wire dimension and E-glass braiding thickness was defined for the practice coil. 615 turns were wound around a pole piece, 3D-printed in Acura Bluestone Epoxy. Dry winding comes with the challenge of maintaining the large number of turns in position as the coil winding progresses. Outer diameter surface definition tooling called "horns" and end caps (Fig. 5) as well as azimuthal clamps were developed and used during the conductor winding.

The coil will be vacuum-impregnated using epoxy CTD 101 K. The curing temperature will be 125 degree C. The material of the practice coil pole piece has been chosen to withstand such temperature. The Formvar coating on the NbTi wire is also compatible with that curing temperature. The impregnation tooling was designed and is being fabricated out of 6061-T6 Aluminum alloy. Following impregnation, the coil will be sectioned to evaluate the quality of the impregnation.

VI. Conclusion

The design of the 28 GHz ECR ion source magnet for FRIB is presented. Its magnetic parameters are similar to the VENUS ECR source in operation at LBNL. Enhancements are proposed in terms of support structure: the mechanical structure relies on the shell-based technology providing preload to the sextupole via bladders and keys allowing fine tuning of the preload and disassembly/re-assembly. In terms of coil fabrication, a dry-layout with vacuum epoxy impregnation is proposed and a practice coil is being fabricated at LBNL to confirm the process and design the tooling.

Acknowledgment

The authors would like to thank warmly Thomas Lipton, James Swanson and Matthew Reynolds for their dedicated work and enthusiasm on this project as well as Charles Swenson for the very fruitful technical discussions.

References

[1] E. Pozdeyev *et al.*, “Status of the FRIB front end,” in *Proc. PAC*, Pasadena, CA, USA, 2013, pp. 734–736.

[2] D. Leitner *et al.*, “Status report and recent developments with VENUS,” in *Proc. ECRIS*, Chicago, IL, USA, 2008, pp. 1–7. [Online]. Available: http://epaper.kek.jp/ecris08/papers/proceedings.pdf

[3] W. Lu *et al.*, “Operation status of SECRAL at IMP,” in *Proc. IPAC*, San Sebastian, Spain, 2011, pp. 1750–1752. [Online]. Available: http://inspirehep.net/search?p=773__w:C11-09-04%20or%20773__w:C11/09/04%20and%20980__a:ConferencePaper

[4] T. Nakagawa, “Recent developments of RIKEN 28 GHz SC-ECRIS,” presented at the ECRIS, Nizhny Novgorod, Russia, 2014.

[5] S. Caspi *et al.*, “The use of pressurized bladders for stress control of superconducting magnets,” *IEEE Trans. Appl. Supercond.*, vol. 11, no. 1, pp. 2272–2275, Mar. 2001.

[6] P. Ferracin *et al.*, “Mechanical behavior of HQ01, a Nb3Sn accelerator-quality quadrupole magnet for the LHC luminosity upgrade,” *IEEE Trans. Appl. Supercond.*, vol. 22, no. 3, Jun. 2012, Art. ID. 4901804.

[7] G. Ambrosio *et al.*, “Test results and analysis of LQS03 third long Nb3Sn quadrupole by LARP,” *IEEE Trans. Appl. Supercond.*, vol. 23, no 3, Jun. 2013, Art. ID. 4002204.

[8] C. Lyneis *et al.*, “Concept for a fourth generation electron cyclotron resonance ion source,” *Rev. Sci. Instrum.*, vol. 83, no. 2, 2012, Art. ID. 02A301.

[9] P. Ferracin *et al.*, “Nb_3Sn superconducting magnets for electron cyclotron resonance ion source,” *Rev. Sci. Instrum.*, vol. 81, no. 2, Feb. 2010, Art. ID. 02A309.

[10] T. Thuillier, “Electron Cyclotron Resonance Ion Sources—I,” Cern Accelerator School, Senec, Slovakia, 29/5-8/6, 2012. [Online]. Available: http://cas.web.cern.ch/cas/Slovakia-2012/Lectures/ThuillierI.pdf

[11] M. N. Wilson, “Computer simulation of the quenching of a superconducting magnet,” Rep. RHEL/M151, 1968.

[12] E. Rochepault *et al.*, “3D mechanical analysis of the ECR source magnet for FRIB,” presented at the 23rd Int. Conf. Magnet Technol., Boston, MA, USA, Jul. 2003.